



ISSN: 0975-833X

Available online at <http://www.journalcra.com>

International Journal of Current Research
Vol. 11, Issue, 04, pp.2999-3005, April, 2019

DOI: <https://doi.org/10.24941/ijcr.35085.04.2019>

INTERNATIONAL JOURNAL
OF CURRENT RESEARCH

RESEARCH ARTICLE

INFLUENZA VIRUS VECTORS: STABILITY OF GENERATED RECOMBINANT VIRUS

*Alaa Karkashan, Thi Thu HaoVan and Peter Smooker

School of Applied Science, RMIT University, Plenty Road, Bundoora 3083, Victoria, Australia

ARTICLE INFO

Article History:

Received 19th January, 2019
Received in revised form
24th February, 2019
Accepted 27th March, 2019
Published online 30th April, 2019

Key Words:

Influenza virus vector,
Recombinant virus stability,
Recombinant haemagglutinin protein,
MD simulation, His tag.

*Corresponding author: Alaa Karkashan

Copyright © 2019, Alaa Karkashan et al. This is an open access article distributed under the Creative Commons Attribution License, which permits unrestricted use, distribution, and reproduction in any medium, provided the original work is properly cited.

Citation: Alaa Karkashan, Thi Thu HaoVan and Peter Smooker, 2019. "Influenza virus vectors: Stability of generated recombinant virus", *International Journal of Current Research*, 11, (04), 2999-3005.

ABSTRACT

Evaluating the conformational changes of a modified viral protein could be the first step in generating a successful stable recombinant virus. This study demonstrates the effect of a small epitope addition into the haemagglutinin (HA) protein of the H1N1 influenza virus, which was compared with the wild-type protein. A hexahistidine (His₆) tag was inserted into a selected antigenic domain within the haemagglutinin HA1 subunit of the A/Puerto Rico/8/34 influenza virus. To investigate the stability of the recombinant HA protein, a molecular dynamics (MD) simulation was used for the His₆-HA protein and for the wild-type HA protein under physiological conditions. Analysis of the MD trajectories showed no significant difference in terms of stability between both systems after 100 nanoseconds of the MD simulation. The His₆ tag influenza virus was then successfully generated using the helper virus-based method. The recombinant mRNA was positively detected amongst the wild-type virus population after three passages of the polymerase chain reaction (PCR) detection method. Our findings indicate that addition of a small epitope is less likely to affect virus stability and infectivity for up to several rounds. Finally, an affinity purification trial resulted in an eluted sample with a low virus amount, which most likely represents the isolated His-tagged virus; however, more investigation is required.

INTRODUCTION

Influenza A virus is a member of the Orthomyxoviridae family [1]. It is an enveloped virus and contains a genome composed of eight negative single-stranded RNA segments (ssRNA) [1]. Haemagglutinin (HA) and neuraminidase are the major viral glycoproteins of influenza A that are targeted and detected by antibodies [1]. The influenza virus offers several advantages as an antigen delivery vector, including safety profiles and the virus's ability to induce strong cellular and humoral immune responses [2, 3]. HA is a primary immune target structure for inducing protective immunity [4, 5]. It is composed of three identical monomers that form a cylindrical shape (Isin *et al.*, 2002). Each HA monomer (mature HA) consists of HA1 and HA2 subunits. The HA1 subunit represents the globular head, and it incorporates specific antigenic domains targeted by antibodies [3, 7, 8]. These domains are antigenically variable, and mutations within these sites that accumulate over time result in the antigenic drift of influenza viruses [9, 10]. Foreign epitopes have been inserted within or near these different antigenic sites for immunological analysis [11-14]. The HA protein is a suitable candidate for epitope insertion, as it contains five antigenic sites, and more importantly, these sites can tolerate the insertion of foreign sequences without disturbing the overall function and structure of the generated recombinant HA [5, 15]. This is because these antigenic sites do not have conserved amino acid sequences among different

influenza A virus strains [15]. Prior to experimentation, evaluating the conformational changes of the modified viral protein can be the first step for predicting a successful stable recombinant virus. In this study, a His tag was inserted in a selected antigenic site of the HA. Using a molecular dynamics (MD) simulation, the stability of the recombinant HA was evaluated by comparing it to the stability of the wild-type (wt) HA. MD is a powerful tool for providing information about protein stability, folding and conformational changes at the atomic level, as this information is difficult to obtain through experimentation [16-18]. The main purpose of performing the MD simulation was to investigate whether there is a significant difference between the modified HA and the wt HA in terms of stability at physiological conditions. Furthermore, we attempted to generate an influenza virus incorporating a His₆ tag and examined the persistence of the recombinant virus among the wt virus by performing several passages. Influenza virus replication occurs in the infected cell nucleus, and it results in synthesis of new copies of viral proteins and genes [19]. During the assembly step of progeny virions, the packaging of viral genomes must be selected from a large pool of viral and host genetic materials [19, 20]. The packaging process involves recognition and selection by a *cis*-acting signal or so-called "packaging signals", which are believed to exist in the coding and non-coding regions of each of the viral RNAs [19, 21]. One factor that could affect the segment-specific packaging signals is mutation, and therefore, the

vRNA may not be selected for virion packaging [22]. Thus, we have examined if the HA incorporating a His tag would still be selected and incorporated into progeny virions along with the remaining vRNAs. Here, we have demonstrated the effect of His₆ tag insertion on the stability of the HA protein using an MD simulation. Then, we generated a His tagged influenza virus using the helper virus-based method, and investigated the possibility of the chimeric HA to be continually packaged into progeny virions with the existence of the wt HA during virus propagation. Finally, we examined the possibility of isolating the His tagged virus by affinity purification.

MATERIALS AND METHODS

His tag insertion to HA protein: The HA protein used was the A/Puerto Rico/8/34 (H1N1) influenza virus (PR8). The nucleotide and amino acid sequences of the HA gene from PR8 in the mRNA sense were obtained from the NCBI sequence database (Gene Bank accession no. EF467821.1). DNA encoding the His₆ tag caccaccaccaccac was added after S158. To gain insight into the His tag location, a structure model for HA-His₆ was built using the Swiss-Model Workspace [23]. The generated structure model was visualized using Visual Molecular Dynamics software (VMD) [24]. The I-TASSER approach was then used to analyse selected profiles of the predicted secondary structure [25, 26].

Molecular dynamics simulation: Many aspects of biomolecular structure, such as protein stability, folding and conformational changes, can be revealed by studying their internal motion [16]. Obtaining dynamic information about, not simply the static structure of, a protein of interest should be considered when analysing the effect of the addition of a foreign epitope to a particular protein [27]. An MD simulation was performed at physiological conditions to compare the stability of the HA after the poly-His tag addition to the stability of the wild-type. The simulation system used was the classical MD with GROMACS version 4.6.3, and the CHARMM36 force field was used to perform the calculations required to build the simulation system. Both proteins, HA-His₆ and wt HA, were simulated at 310 K for 100 ns. Therefore, two sets of trajectories were obtained using GROMACS. Before the simulations were run, a cubic water box was constructed with selected proportions to solvate the proteins. Water molecules were gradually added in the box until the water density reached $\sim 1.0 \text{ g/cm}^3$ and the models were covered. Counter ions (Cl⁻) were then added to neutralize the system. Afterward, the Steepest Descent energy minimization method was performed to reach the lowest possible local energy point. The system was equilibrated using a Bussi coupling thermostat and Parrinello-Rahman coupling barostat to maintain the temperature at 310 K and pressure at 1 atm [28, 29]. Time steps of 2 ps were used to integrate the equation of motion, and the simulation was updated every 10 steps. At the end of the simulation, the stability of the His tag HA protein was compared to that of the wtHA protein by analysing the MD trajectories.

Construction of the plasmid: The cDNA sequence encoding the His tagged viral RNA of the PR8 virus was inserted in the antisense orientation [30] between the canine RNA polymerase I promoter [31] and the mouse RNA polymerase I terminator [32, 33] sequences. The coding sequence of the designated HA-His₆ pol I construct was generated synthetically

(Genscript). The construct was cloned into the pRNA-CMV3.1/Neo plasmid vector (Genscript) using the restriction sites *NdeI* and *HindIII*. Accordingly, these restriction enzyme sites were included in the HA-His₆ pol I construct at the 5' and 3' ends. The constructed plasmid will be referred to as pCDNA/HAPR8-His₆ pol I.

Cells and virus: Madin Darby Canine Kidney cells (MDCK, Sigma-Aldrich, Germany) were used for the propagation of the PR8 virus and for the transfection and generation of the recombinant influenza virus. MDCK cells were maintained in Dulbecco's modified Eagle medium (DMEM, Gibco, USA) supplemented with 10% foetal bovine serum (FBS, Gibco) and 100 U/ml penicillin-streptomycin. Cells were incubated at 37°C with 5% CO₂ in a humidified incubator. For propagating the PR8 virus, the cell growth culture medium was replaced with a virus growth medium (VGM). The VGM consisted of DMEM supplemented with 0.2% BSA (bovine albumin fraction V 7.5%, Gibco, USA), 2 µg/mL TPCK-trypsin (Sigma-Aldrich, Germany) and 100 U/ml penicillin-streptomycin. Cells were infected with 1:1000 diluted virus stock (original HA titre = 6400) after reaching approximately 80% confluence. Cells were incubated for up to 4 days at 37°C with regular observation for the cytopathic effect (CPE). The culture medium of the infected cells was then harvested and centrifuged at 3,000 *x g* for 3 min to remove cell debris. Virus purification was performed with ultracentrifugation for 2 h (28,000 *x g* at 4°C in an Optima L-80 XP Beckman rotor Ti-41) through a 20% sucrose cushion. The virus pellet was resuspended in 20 µL TNE buffer (50 mM Tris, 140 mM NaCl, 5 mM EDTA) after removing the medium and sucrose cushion.

Production of recombinant influenza virus: pCDNA/HAPR8-His₆ pol I plasmid was transfected into the MDCK cells using the lipofectamine[®] 2000 transfection reagent (Invitrogen, USA). Briefly, 5 × 10⁴ MDCK cells were seeded in a 24-well tissue culture plate so that the cells were approximately 90% confluent at the time of transfection. Cells were maintained in an antibiotic free DMEM medium supplemented with 10% FBS and were incubated at 37°C with 5% CO₂. After 24 h, the cell culture medium was replaced with a serum-free medium. In all, 0.8 µg of plasmid DNA and 2 µL of the transfection reagent were diluted in 50 µL of Opti-MEM[®] (Gibco, USA) separately and incubated for five minutes at RT. Then, the two mixtures were combined and incubated for a further 20 min at RT. The transfected cells were incubated for 24 h at 37°C with 5% CO₂. For co-infection with the PR8 helper virus, the cell culture media was replaced with VGM without antibiotics. Cells were infected with the helper PR8 virus (wild-type PR8) at MOI 0.1 and incubated for 48 hours at 37°C with 5% CO₂. The culture medium was then transferred into 75 cm² tissue culture flasks previously seeded with cells to obtain a higher virus titre. Flasks were incubated for up to four days or until the maximum CPE was observed. Subsequently, virus purification through a 20% sucrose cushion and haemagglutination assay [34] were performed.

Persistence of the recombinant virus among the wild-type virus: The ability of the His tagged virus to persist with the wild-type virus was investigated. The generated virus mixture (recombinant and wt viruses) from the reverse genetics (Caton and Brownlee) was passaged for three rounds. The virus re-propagation was performed in MDCK cells as described previously. The presence of the recombinant virus was confirmed by RT-PCR as described in the following section.

RT-PCR amplification of the recombinant HA segment:

Total RNA of the PR8 virus was extracted using "Isolate II RNA Mini kit" (Bioline, Australia) according to the manufacturer's instruction. Three viral samples were used for the RNA extraction: the wt PR8, the virus mixture generated from RG and the fourth-generation virus mixture propagated from RG. Reverse transcription was carried out using the ThermoScript RT-PCR system (Invitrogen, USA). Briefly, 9 μ L of extracted RNA (between 100 to 350ng) was mixed with 1 μ Loligo (dt)₂₀, 2 μ L of 10 mMdNTP mix to a final volume of 12 μ L. The RNA was denatured by incubating at 65°C for five minutes. A master mix was then prepared and was mixed with the previous reaction according to the manufacturer's instruction. The cDNA was synthesised at 50°C for 50 min, and the reaction was terminated at 85°C for 5 min. The PCR reaction was performed by adding 1-3 μ LcDNA (<200 ng) to a reaction mixture containing 12.5 μ Lof Go Taq[®] Green Master Mix (1x, Promega, USA) and 1 μ L of each primer (0.4 μ m): His₆ forward CACCACCACCACCACAGT and His₆ reverse CCTCCCAGCTTGATCTCTTACTTTG. The final reaction volume was adjusted to 25 μ L by adding Nuclease-free water. The amplification was performed on a G-Storm GS1 Thermo cycler (G-Storm, UK). After initial denaturation at 95°C for 1 min, the reactions were cycled 35 times at 95°C/15 sec for denaturation, 55°C/15 sec for annealing and 72°C/15 sec for elongation. The obtained PCR fragment was analysed on a 1.5% agarose gel stained with ethidium bromide.

Batch affinity isolation: In all, 150 μ L of pre-charged 50% Ni-NTA agarose (Invitrogen, USA) was loaded into a microcentrifuge tube. The resin was washed twice with 20 mM binding buffer [0.50 mL 2 M imidazole, pH 7.4 (GE Healthcare, Sweden); 6.25 mL of phosphate buffer stock solution (PBS), pH 7.4 (GE Healthcare, Sweden); and up to 50 mL of dH₂O] and was centrifuged for 3 min at high speed. A total of 100 μ L of the purified virus sample (generated from RG) was diluted with 100 μ L of 20 mM binding buffer and was added to the resin. The virus-resin mixture was incubated for two hours at 4°C with agitation. The mixture was then centrifuged at high speed for 2 min, and the supernatant was removed and saved for analysis. Then, 75 μ L of 50 mM washing buffer [1.25 mL of 2 M imidazole, pH 7.4 (GE Healthcare, Sweden); 6.25 mL of PBS, pH 7.4; and up to 50 mL dH₂O] was added and centrifuged for 1 min at high speed. The washing step was repeated three times and the washed solution was saved for analysis. Finally, a 50 μ L of 500 mM elution buffer [12.50 mL of 2 M imidazole, pH 7.4; 6.25 mL of PBS, pH 7.4; and up to 50 mL of dH₂O] was added and incubated for five minutes at RT. The tube was centrifuged at high speed for one minute, and the supernatant (eluted sample) was collected. Samples were loaded into 12% polyacrylamide gels and stained with Acqua Stain (Bulldog Bio Inc., USA).

RESULTS

HA-His₆ protein structure model: The structure of the wt HA (before His₆ addition) and HA-His₆ were obtained (Fig. 1). HA is a homotrimer, and each monomer consists of two subunits: HA1 and HA2 (blue and red structures in Fig. 1 respectively). The His₆insertion site is located within an external loop of the HA1 subunit. The addition of the His tag formed a coiled secondary structure between S158 and S159 (Fig. 1A), with a confidence score ranging between 5 and 7 predicted by the I-TASSER server (data not shown).

Moreover, the B-factor profile (BFP, or so called normalized B-factor) was obtained using I-TASSER. It is an important indicator of the protein's structure, and indicates its dynamics and flexibility [35]. Residues with negative or close to zero BFP values are often structurally more stable, whereas BSP values higher than zero are more flexible [26, 36]. BFPs for amino acids (Fig. 2) 158-165 from the His tagged protein were predicted as follows: 0.86, 1.49, 2.51, 1.77, 1.76, 0.64, 0.10, and -0.52, respectively [36].

Molecular dynamics trajectory analysis: As seen from observation of the overall behaviour of the wt and recombinant HA proteins, addition of the His tag did not affect the general HA structure (with respect to the observed motion). The trajectories were analysed using VMD [24]. To investigate the protein mobility and the associated changes, root mean square fluctuations (RMSFs) for all side chain atoms of each residue were calculated. RMSFs of the average atomic mobility for the His₆-HA and wt HA are shown in Fig. 3. RMSFs fluctuated in a similar manner for both HAs. However, the His₆-HA had slightly larger RMSF values than the wt HA. Residues around the His₆ (residues 157 and 177) had relatively larger RMSF values than the other domains. The root mean square deviation (RMSD) is a commonly used quantitative measure for the conformational similarity and stability between two or more related protein structures [37, 38]. RMSD plots were calculated during the course of the MD simulation and the stability of the simulation was evaluated based on the RMSD. The RMSD plots of the trajectories of the HA-His₆ (red curve) and the wt HA (blue curve) are illustrated in Fig. 3. The plots show a moving average of 100 ns to allow for effective assessment of the overall trends between the two systems. RMSD was performed on the backbone atoms of the entire HA molecule for both systems. Within the first few nanoseconds, a quick RMSD jump was observed, which was due to the initial relaxed condition of the starting model. RMSD for the HA-His₆ was slightly smaller than that of the wt HA system. With both systems, a relatively small fluctuation in RMSD values was observed, and the trajectories stabilized over the time course. Both systems had reached equilibrium after 80 ns and became stable with a RMSD value of ~5 Å.

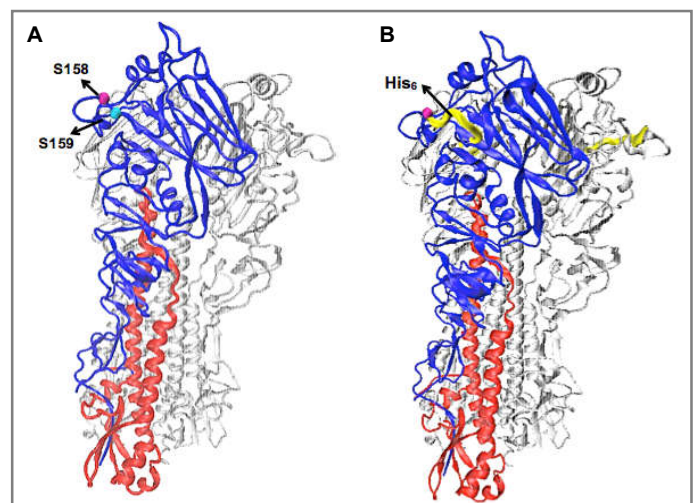


Figure 1. Structure of HA protein with one monomer highlighted in colours. The HA1 and HA2 subunits are represented with structures coloured blue and red respectively. A) HA protein before His₆ addition. The selected insertion site is between S158 (cyan bead) and S159 (magenta bead). B) HA protein after His₆ addition. The His tag is represented as the coil structure coloured by yellow

HA-His₆ encoding vector: The designed HA-His₆ pol I construct is illustrated in Fig. 4A. The His tag was inserted within the HA1 subunit of the HA (represented by red bar and nucleotide sequence). The pRNA-CMV3.1/Neo plasmid vector that was used for cloning the synthesised HA-His₆ pol I construct has the CMV promoter. Part of this promoter was substituted by the cloned construct, and therefore, it was inactivated (Fig. 4B). The final constructed plasmid, pCDNA/HAPR8-His6 pol I that was used for generating the recombinant influenza virus is shown in Fig. 4C. The correct insert was confirmed by digesting the plasmid with *NdeI* and *HindIII* restriction enzymes (result not shown). The expected fragment sizes for the digested DNA were 4783 bp and 2450 bp.

Generation of the recombinant influenza virus incorporating a His tag: After 48 hours from infection with the helper virus, CPE was observed on more than 80% of the MDCK cells (typical CPE by influenza viruses include rounding up and detachment of infected cells from the tissue culture plate). The culture media of the infected cells was passaged from the cell culture well into a 75 cm² tissue culture flask. Four days later, approximately 80% of the cells showed CPE. The titre obtained for the purified virus sample using the haemagglutination assay was 1600, and the HA titre for the virus sample that was propagated after three passage rounds was 1600. The presence of the His tagged virus was confirmed by RT-PCR. The expected size of the amplified region containing the His tag was 269 bp. From the PCR results shown in Fig. 5, presence of the recombinant viral mRNA was successfully observed. The correct bandsize was only visualized on the agarose gel with the virus samples that were expected to contain the generated His tagged virus (virus produced from the RG with the helper virus and the virus produced from the RG were passaged for three rounds).

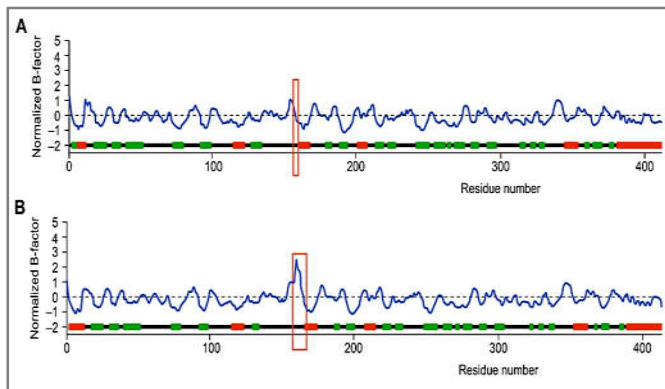


Figure 2. B-factor profile (BFP) predicted by I-TASSER server. A) BFP for the wt HA protein. B) BFP for the His₆-HA protein. The two serine amino acids (S158 and S 159) before the 6 x His tag addition and after the 6x His tag addition are indicated with the orange box.

Isolation of the His tag virus by batch purification: The supernatant that was separated from incubation of the virus-resin mixture, the solution saved from all three washing steps and the eluted sample were loaded into a 12% SDS gel. After protein separation (Fig. 6), the viral protein bands from the supernatant sample were the highest in intensity compared to the other samples (with exception to the virus sample loaded as a control). The band intensity indicates the quantity of the viral proteins available within the loaded sample, hence, the amount of the virus.

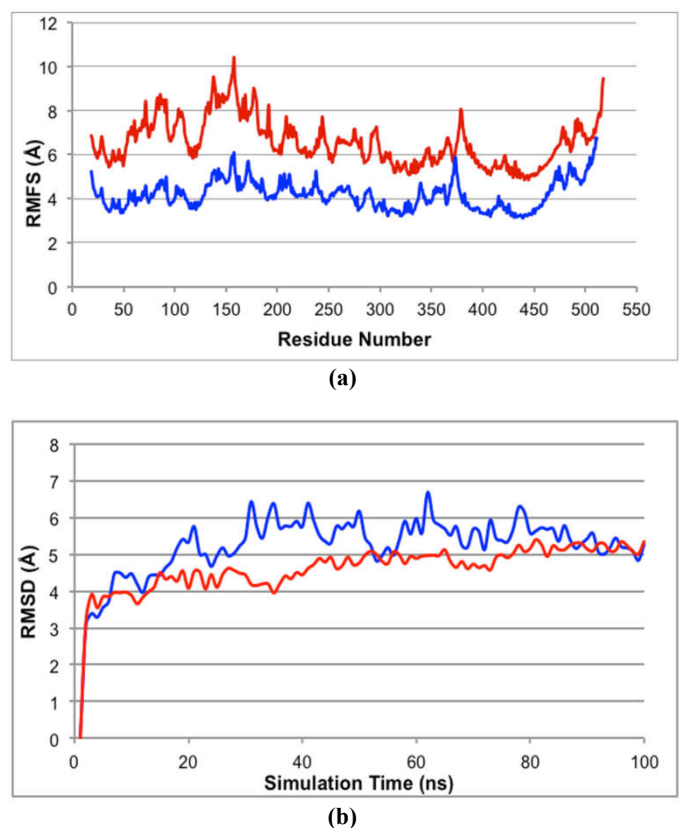


Figure 3. Comparison of the His₆-HA and wt HA proteins by molecular dynamics simulation. A) RMSF for all the side-chain atoms of the wt HA system (blue) and the His₆-HA system (red). B) RMSD for all backbone atoms of the wt HA system (blue) and the His₆-HA system (red)

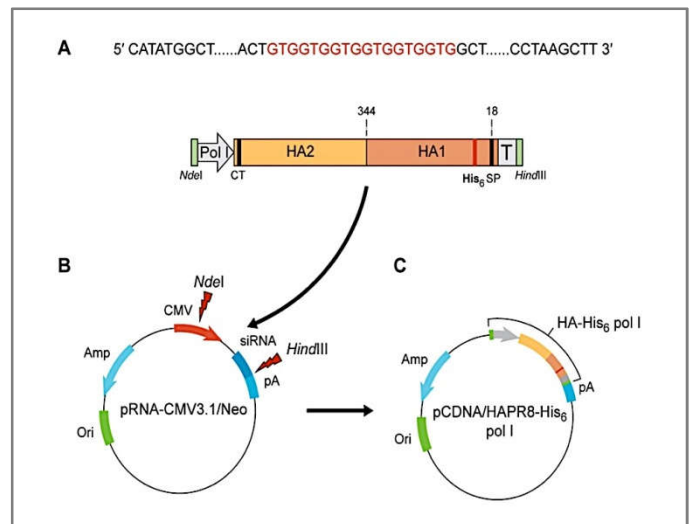


Figure 4. Construction of the pCDNA/HAPR8-His₆ pol I plasmid used to generate the recombinant influenza virus. A) Schematic presentation of the HA-His₆ pol I construct. cDNA encoding the recombinant HA is in the antisense orientation between the canine pol I promoter (Pol I) and the mouse pol I terminator (T). The nucleotide sequence in red represents the His tag. Cytoplasmic tail (CT), signal peptide (SP). B) The pRNA-CMV3.1/Neo plasmid used for cloning the HA-His₆ pol I construct with *NdeI* and *HindIII* sites. C) The pCDNA/HAPR8-His₆ pol I plasmid containing the HA-His₆ pol I construct.

The virus quantity decreased with the three washes and had almost disappeared in the third wash. With the eluted virus sample, faint bands for the viral proteins were observed, which most likely represents the isolated His tagged virus.

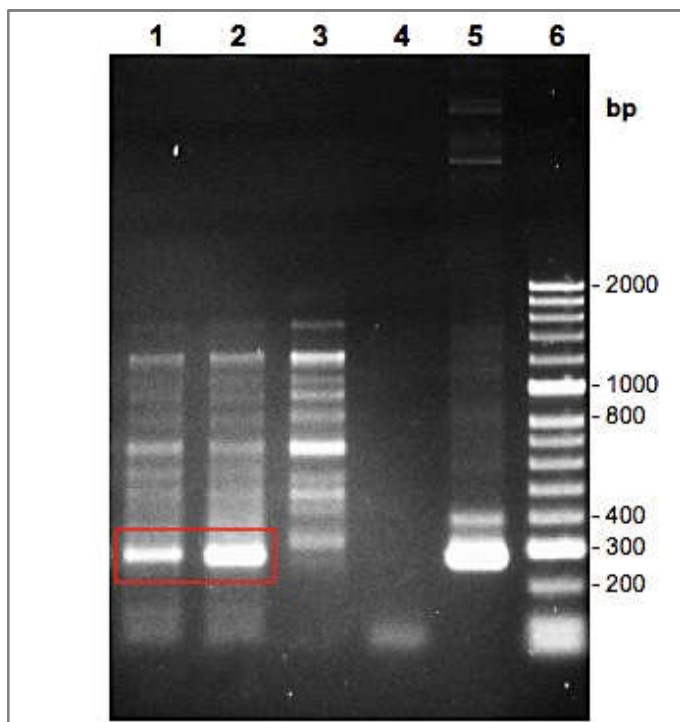
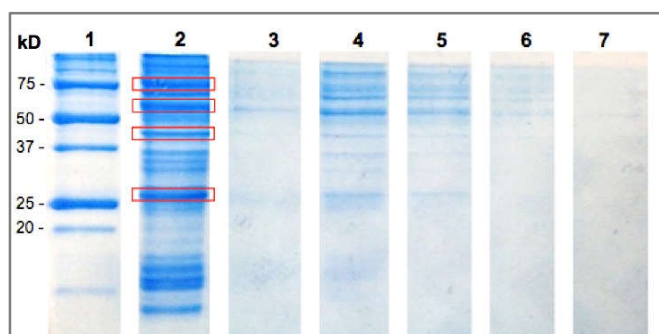


Figure 5. RT-PCR detection of the His tagged influenza virus. The region containing the His₆ tag of the recombinant mRNA was amplified using specific primers. The size of the expected amplified region is 269 bp. The bands marked with the red box represent the correct amplified size within the examined virus samples. Lane 1: virus generated from the RG with the helper PR8 virus, lane 2: virus produced from RG and passaged for three rounds, lane 3: wild-type PR8 virus (-ve), lane 4: water, lane 5: pCDNA/HAPR8-His₆ pol I plasmid, lane 6: Hyperladder™ II marker.



* Protein band assignments based on literature data [7, 39-43].

Figure 6. Influenza virus proteins separated with SDS-PAGE after affinity batch purification. Virus samples contained a combination of wild-type PR8 and His tagged PR8 viruses (obtained from the RG experiment) and were loaded into a 12% polyacrylamide gel and stained with Coomassie instant staining. The protein bands marked with the red box may represent uncleaved HA0 (~ 75 kDa*), NP (~ 60 kDa*) and HA1 (~ 42-46 kDa*) and HA2 (27 kDa*) subunits. Lane 1: protein marker. Lane 2: virus samples from reverse genetics experiment (before batch purification), lane 3: eluted sample, lane 4: supernatant sample after virus incubation with the resin, lane 5: 1st washed sample, lane 6: 2nd washed sample, lane 7: 3rd washed sample.

DISCUSSION

Advances in the fields of genetic engineering and molecular biology have enabled the development of live vector vaccines [44]. Influenza viral vectors offer many advantages as a vaccine delivery vehicle, such as the ability to induce strong

immune responses [2]. The licensed influenza vaccine strains provide a major advantage, as they can serve as a safe vaccine delivery vector [2]. Predicting the stability of an influenza virus incorporating a foreign insert can significantly assist with designing and then producing a genetically stable recombinant virus. In this study, we investigated the stability of HA incorporating a His₆ tag and compared the structural variation with the wt HA using MD simulation. Later, we experimentally generated a recombinant influenza virus and examined its ability to persist during virus propagation along with the wt virus. The S158 amino acid residue that was selected for insertion of the His₆ tag has been identified within the Ca2 antigenic region of H1 subtype of viruses, which is known to be from the accessible hypervariable region [7, 45]. Many studies have revealed that most of the antigenic epitopes contain highly flexible, protruding loops, and shape changing might not alter the virus stability, with the exception of the antigenic sites Ca1 and [46, 47]. As shown in Fig. 1, His₆ addition resulted in a protruded structure between S185 and S159 based on the Swiss-Model prediction. To undertake flexibility prediction, we used the I-TASSER server for predicting the BFP. The BFP prediction uses a combination of template-based assignment, protein structure and sequence profiles [48].

The BFP scores suggest that the His tag region was slightly more flexible (less stable) when compared to the overall predicted normalized B-factor for the HA structure (Fig. 2). The highest score predicted was 2.51 and that was for H160. As a comparison, the scores obtained for S158 and S159 were 0.15 and -0.37, respectively, before addition of the His tag, and these scores changed to 0.86 and -0.52, respectively, with the His tag addition. Analysis of the scores obtained for both generated systems indicates that the changes caused by addition of the His tag to the flexibility of the HA structure, particularly the His₆ region, were not considered to be significant. To determine whether the addition of a foreign epitope (His₆) could affect the dynamic behaviour of HA, RMSF were analysed. The RMSF values obtained (Fig. 3) indicate that the addition of His₆ made the HA protein somewhat more flexible than the wt HA. Moreover, the fluctuating magnitudes for some of the residues in the His tag region were larger than others within the His₆-HA protein. This was in agreement with the BFP scores predicted for this modified region. RMSD is one of the key parameters used to predict and evaluate the stability of proteins [27]. As seen in Fig. 3, RMSD trajectory values for the His₆-HA between 10 ns and 80 ns were slightly lower than that of the wt HA. This suggests that His₆-HA was more stable than the wt HA at the start of the simulation time period. Overall, there were no significant differences between the His₆-HA and wt HA systems in terms of stability and conformational changes. Previous experimental studies showed that expression of foreign peptides, as part of the viral protein, did not affect viral infectivity [11, 12, 21, 49]. Our computational study is in agreement with these studies, as the stability of the recombinant HA did not differ from that of the wt HA. The second part of our study involved generation of the recombinant influenza virus. Recombinant influenza virus carrying a His₆ tag was successfully generated using the pol I method with the helper virus. The presence of the tagged virus was confirmed by detecting the recombinant mRNA HA using the PCR technique. Packaging of the His tagged HA vRNA into progeny recombinant virus was sustained among the progeny wild-type virus production. The presence of the recombinant HA mRNA was detected by PCR within the

fourth generation of viruses (passage 3). In an earlier study, recombinant plasmid encoding the NS gene was constructed by replacing the NS coding region with the CAT(chloramphenicol acetyltransferase) gene [50]. The foreign recombinant gene was packaged into viral particles with the use of a helper virus and was passaged successfully several times. However, detection of the recombinant gene expression (CAT activity) was then rapidly lost among the helper virus after further passages [50]. In another study, recombinant influenza virus expressing the HPV16 oncogene was generated using the plasmid reverse genetics system [51]. The stability of the transgene within the recombinant influenza virus was confirmed by passaging the virus for up to 5 rounds [51]. It can be hypothesized from these two studies that the presence of the wt virus (helper virus) may lead to a gradual loss of the recombinant gene during virus passaging. This could be because the presence of the viral wtvRNA can compete with the recombinant one for selection during viral packaging, possibly due to bundling signals [52]. However, having a pure recombinant virus population will not cause this issue with virus replication, as the only gene type available for packaging is the recombinant one. Moreover, replacing the whole coding region with a foreign gene can affect the recognition and selection of the packaging signals that are believed to exist in both coding and non-coding regions [19, 21]. Consequently, this can possibly affect the continued packaging of the recombinant viral segment.

Affinity batch purification was conducted to examine whether the His tagged viruses could be isolated from the non-tagged virus, which could be practical for future applications. The eluted sample from the purification contained a low virus amount that was indicated by the result observed on the SDS gel (Fig. 6). Generating recombinant influenza virus with the use of helper virus based method will result in progeny viruses of which the large majority are helper viruses [53]. The isolated virus within the eluted sample probably represents the His tagged virus, however more investigation is required in order to confirm this, as well as to estimate the sample purity. In conclusion, the stability of the HA protein incorporating a foreign epitope (His₆tag) within a selected antigenic domain was demonstrated via MD simulation. The recombinant influenza virus was then successfully generated using the helper virus-based reverse genetics system. Additionally, the recombinant virus was able to persist for several passages amongst the wild-type virus. Thus, using the influenza virus as a vaccine vector is a promising approach. Investigations that were undertaken in this study can provide insight into the effect of small foreign epitope insertion on HA dynamics and stability, which in turn could provide new knowledge in the field of recombinant influenza viruses.

Conflict of interest: The authors declare no financial or commercial conflict of interest.

Acknowledgements: We thank Dr. Xiaozheng Mu for performing the molecular dynamics simulation.

References

- Iwasaki, A. and Pillai, P. S. 2014. Innate immunity to influenza virus infection. *Nat. Rev Immunol*, 14(5), 315-28.
- Stukova, M. A. et al. 2006. Vaccine potential of influenza vectors expressing Mycobacterium tuberculosis ESAT-6 protein. *Tuberculosis (Edinb)*, 86(3-4), 236-46.
- Martinez-Sorbido, L. & Garcia-Sastre A. 2007. Recombinant influenza virus vectors. *Future Virol*, 2, 401-416.
- Neumann, G. and Kawaoka, Y. 2002. generation of influenza A virus from cloned cDNAs-historical perspective and outlook for the new millennium. *Rev Med Virol*, 12,13-30.
- Sriwilaijaroen, N. and Suzuki, Y. 2012. Molecular basis of the structure and function of H1 hemagglutinin of influenza virus. *Proc. Jpn. Acad. Ser. B Phys. Biol Sci*, 88(6), 226-249.
- Isin, B., Doruker, P. and Bahar, I. 2002. Functional motions of influenza virus hemagglutinin: a structure-based analytical approach. *Biophys J*, 82(2), 569-581.
- Caton, A. J. and Brownie, G. G. 1982. The antigenic structure of the influenza virus A/PR/8/34 hemagglutinin (H1 subtype). *Cell*, 31, 417-427.
- Wilson, I. A. and Cox, N. J., (1990. Structural basis of immune recognition of influenza virus hemagglutinin. *Annu Rev Immunol*, 8, 737-71.
- Soundararajan, V. et al. 2011. Networks link antigenic and receptor-binding sites of influenza hemagglutinin: Mechanistic insight into fitter strain propagation. *Sci Rep*, 1.
- Ellebedy, A. H. and Ahmed, R. 2012. Re-engaging cross-reactive memory B Cells: The influenza puzzle. *Front Immunol*, 3, 53.
- Thomas, P. G., Brown, S. A., Yue, W., So, J., Webby, R. J. and Doherty, P. C. 2006. An unexpected antibody response to an engineered influenza virus modifies CD8+ T cell responses. *PNAS*, 103(8), 2764-9.
- Gilleland, H. E. et al. 2000. Chimeric animal and plant viruses expressing epitopes of outer membrane protein F as a combined vaccine against Pseudomonas aeruginosa lung infection. *FEMS Immunol Med Microbiol.*, 27(4): p. 291-7.
- Li, Z. N. et al. 2005. Chimeric influenza virus hemagglutinin proteins containing large domains of the Bacillus anthracis protective antigen: protein characterization, incorporation into infectious influenza viruses, and antigenicity. *J Virol*, 79(15), 10003-12.
- Garulli, B., Di Mario, G., Sciaraffia, E., Kawaoka, Y. and Castrucci, M. R. (2011. Immunogenicity of a Recombinant Influenza Virus Bearing Both the CD4+ and CD8+ T Cell Epitopes of Ovalbumin. *J. Biomed Biotechnol*, 2011, 497364.
- Garcia-Sastre, A. 2000. Transfectant influenza viruses as antigen delivery vectors. *Adv Virus Res*, 55, 579-97.
- Adcock, S.A. and McCammon, J. A. 2006. Molecular Dynamics: Survey of Methods for Simulating the Activity of Proteins. *Chem. Rev*, 106(5), 1589-1615.
- Lindahl, E.R. 2008. Molecular dynamics simulations. *Methods Mol Biol*, 443, 23.
- Wang, Y. et al. 2013. Insight into the structural stability of wild type and mutants of the tobacco etch virus protease with molecular dynamics simulations. *J Mol Model*, 19(11), 4865-75.
- Watanabe, T., Watanabe, S., Noda, T., Fujii, Y. and Kawaoka, Y. 2003. Exploitation of Nucleic Acid Packaging Signals To Generate a Novel Influenza Virus-Based Vector Stably Expressing Two Foreign Genes. *J Virol*, 77(19), 10575-10583.
- Noda, T. and Kawaoka, Y. 2012. Packaging of influenza virus genome: robustness of selection. *PNAS*, 109(23), 8797-8.
- Li, F. et al. 2010. Generation of replication-competent recombinant influenza A viruses carrying a reporter gene

- harbored in the neuraminidase segment. *J Virol*, 84(22), 12075-81.
22. Hutchinson, E. C., von Kirchbach, J. C., Gog, J. R. and Digard, P. 2010. Genome packaging in influenza A virus. *J Gen Virol*, 91(Pt 2), 313-28.
 23. Arnold, K., Bordoli, L., Kopp, J. and Schwede, T. 2006. The SWISS-MODEL workspace: a web-based environment for protein structure homology modelling. *Bioinformatics*, 22(2), 95-201.
 24. Humphrey, W., Dalke, A. and Schulten, K. 1996. VMD: visual molecular dynamics. *J Mol Graph*, 14(1), 33-8, 27-8.
 25. Roy, A., Xu, D., Poisson, J. and Zhang, Y. 2011. A Protocol for Computer-Based Protein Structure and Function Prediction. *J Vis Exp*, 3(57), e3259.
 26. Yang, J., Yan, R., Roy, A., Xu, D., Poisson, J. and Zhang, Y. 2015. The I-TASSER Suite: protein structure and function prediction. *Nat Meth*, 12(1), 7-8.
 27. Li, X. B., Wang, S. Q., Xu, W. R., Wang, R. L. and Chou, K. C. (2011). Novel inhibitor design for hemagglutinin against H1N1 influenza virus by core hopping method. *PLoS One*, 6(11), e28111.
 28. Parrinello, M. and Rahman, A. (1980). Crystal Structure and Pair Potentials: A Molecular-Dynamics Study. *Phys Rev Lett*, 45(14), 1196-1199.
 29. Bussi, G., Donadio, D. and Parrinello, M. 2007. Canonical sampling through velocity rescaling. *J Chem Phys*, 126(1), 014101.
 30. Neumann, G. *et al.* 1999. Generation of influenza A viruses entirely from cloned cDNAs. *PNAS*, 96(16), 9345-50.
 31. Murakami, S., Horimoto, T., Yamada, S., Kakugawa, S., Goto, H. and Kawaoka, Y. 2008. Establishment of canine polymerase I-driven reverse genetics for influenza A virus: its application for H5N1 vaccine production. *J Virol*, 82, 1605-1609.
 32. Grummt, I., Maier, U., Ohrlein, A., Hassouna, N. and Bachellerie, J. P. 1985. Transcription of mouse rDNA terminates downstream of the 3' end of 28S RNA and involves interaction of factors with repeated sequences in the 3' spacer. *Cell*, 43(3 Pt 2), 801-10.
 33. Neumann, G., Zobel, A. and Hobom, G. 1994. RNA polymerase I-mediated expression of influenza viral RNA molecules. *Virology*, 202(1): 477-9.
 34. Klimov, A. *et al.* 2012. Influenza virus titration, antigenic characterization, and serological methods for antibody detection. *Methods Mol Biol*, 865, 25-51.
 35. Yuan, Z., Bailey, T. L. and R. D. Teasdale, (2005). Prediction of protein B-factor profiles. *Proteins*, 58(4), 905-12.
 36. Yang, J., Wang, Y. and Zhang, Y. 2016. ResQ: An Approach to Unified Estimation of B-Factor and Residue-Specific Error in Protein Structure Prediction. *J Mol Biol*, 428(4), 693-701.
 37. Lee, H. S., Qi, Y. and Im, W. 2015. Effects of N-glycosylation on protein conformation and dynamics: Protein Data Bank analysis and molecular dynamics simulation study. *Sci Rep*, 5, 8926.
 38. Kufareva, I. and Abagyan, R. 2012. Methods of protein structure comparison. *Methods Mol Biol*, 857, 231-57.
 39. Yewdell, J. W., Yellen, A. and Bachi, T. 1988. Monoclonal antibodies localize events in the folding, assembly, and intracellular transport of the influenza virus hemagglutinin glycoprotein. *Cell*, 52(6), 843-52.
 40. Palamara, A. T. *et al.* 2005. Inhibition of influenza A virus replication by resveratrol. *J Infect Dis*, 191(10), 1719-29.
 41. Shaw, M. L., Stone, K. L., Colangelo, C. M., Gulcicek, E. E. and Palese, P. 2008. Cellular proteins in influenza virus particles. *PLoS Pathog*, 4(6), e1000085.
 42. Hsu, B. B., Yinn Wong, S., Hammond, P. T., Chen, J. and Klibanov, A. M. 2011. Mechanism of inactivation of influenza viruses by immobilized hydrophobic polycations. *PNAS*, 108(1), 61-6.
 43. Abdoli, A. *et al.* 2014. An H1-H3 chimeric influenza virosome confers complete protection against lethal challenge with PR8 (H1N1) and X47 (H3N2) viruses in mice. *Pathog Dis*, 72(3), 197-207.
 44. Nascimento, I. P. and Leite, L. C. C. 2012. Recombinant vaccines and the development of new vaccine strategies. *Braz J Med Biol Res*, 45(12), 1102-1111.
 45. Xu, R., Krause, J. C., McBride, R., Paulson, J. C., Crowe, J. E., Jr., and Wilson, I. A. 2013. A recurring motif for antibody recognition of the receptor-binding site of influenza hemagglutinin. *Nat Struct Mol Biol*, 20(3), 363-70.
 46. Xu, R., Ekiert, D. C., Krause, J. C., Hai, R., Crowe, J. E. Jr. and Wilson, I. A. 2010. Structural basis of preexisting immunity to the 2009 H1N1 pandemic influenza virus. *Science*, 328(5976), 357-60.
 47. Stray, S. J. and Pittman, L. B. 2012. Subtype- and antigenic site-specific differences in biophysical influences on evolution of influenza virus hemagglutinin. *Virology*, 9, 91.
 48. Yang, J. and Zhang, Y. 2015. Protein Structure and Function Prediction Using I-TASSER. *Curr Protoc Bioinformatics*, 52, 5.8.1-5.8.15.
 49. Tan, H. X. *et al.* 2016. Recombinant influenza virus expressing HIV-1 p24 capsid protein induces mucosal HIV-specific CD8 T-cell responses. *Vaccine*, 34(9), 172-9.
 50. Luytjes, W., Krystal, M., Enami, M., Parvin, J. D. and Palese, P. 1989. Amplification, expression, and packaging of a foreign gene by influenza virus. *Cell*, 59(6), 1107-1113.
 51. Jindra, C. *et al.* 2015. Attenuated Recombinant Influenza A Virus Expressing HPV16 E6 and E7 as a Novel Therapeutic Vaccine Approach. *PLoS One*, 10(9), e0138722.
 52. Goto, H., Muramoto, Y., Noda, T. and Kawaoka, Y. 2013. The Genome-Packaging Signal of the Influenza A Virus Genome Comprises a Genome Incorporation Signal and a Genome-Bundling Signal. *J Virol*, 87(21), 11316-11322.
 53. Li, J., Arevalo, M. T. and Zeng, M. 2013. Engineering influenza viral vectors. *Bioengineered*, 4(1), 9-14.
